Supporting Information for:

Tailoring of an ultralow temperature adaptive cellulose nanofiber-based flexible zinc-air battery with long cycle life

Yichun Xue,[a, b] Hang Zhou,[a, b] Keyu Wang,[c] Hongxiang Zhu,[*a, b] Linzhou Zhuang,[*c] Zhi Xu [c] and Hui He[*a, b]

[a.] School of Light Industry and Food Engineering, Guangxi University, Nanning 530004, PR China.

[b.] Guangxi Key Laboratory of Clean Pulp & Papermaking and Pollution Control, Nanning 530004, PR China.

[c.] State Key Laboratory of Chemical Engineering, School of Chemical Engineering, East China University of Science and Technology, Shanghai 200237, PR China.

Simulation details

A sodium polyacrylate molecule (PANa) was represented by a 22-residue polymer chain. This molecule is completely deprotonated. The negative charges of the 22 carboxylate groups are compensated by sodium cations. Cellulose molecules consisting of 6 glucose monomers, denoted CNF, were used.

To compare the water absorption characteristics of hydrogels, two hydrogel model systems, CNF/PANa, (6 PANa + 1 CNF-COOH + 8000 H_2O), and CNF/PANa/LiCl (6 PANa + 1 CNF-COOH + 15 LiCl + 8000 H_2O), were built. In all cases, at the beginning of the simulation, the energy of the model system was minimized. After that, a molecular dynamics of 1000 ps at constant temperature (300 K) and pressure (1 atm) (NPT) was performed, which brought the system into a reasonable preequilibrated configuration. After that, a further 2000 ps NVT ensemble molecular dynamics simulation was conducted at 300 K to track changes in the system.

In this work, Packmol was used to build the initial configuration of all the model systems. LAMMPS and PCFF force fields were used to perform the molecular simulations. The time step was fixed at 1.0 fs, and the temperature and pressure were controlled by the Nosé–Hoover thermostat-barostat. A van der Waals interaction cutoff of 1.5 nm was employed, and the PPPM method was used to account for the long-range electrostatic interactions. The atomic coordinates were saved every 1 ps for further analysis.

Model

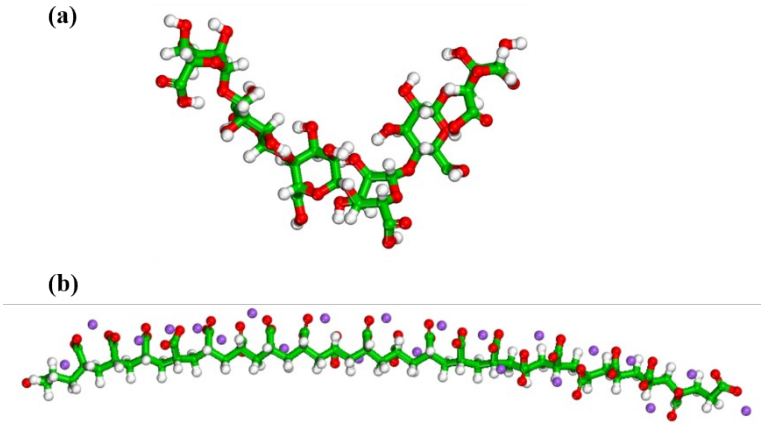

The model of (a) CNF and (b) sodium polyacrylate molecule (PANa).

Figure

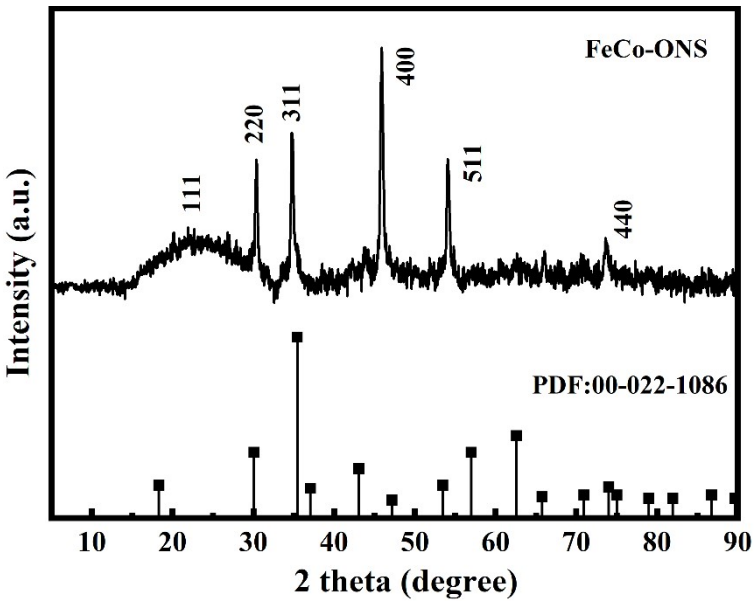

Figure S1. XRD pattern of FeCo-ONS.

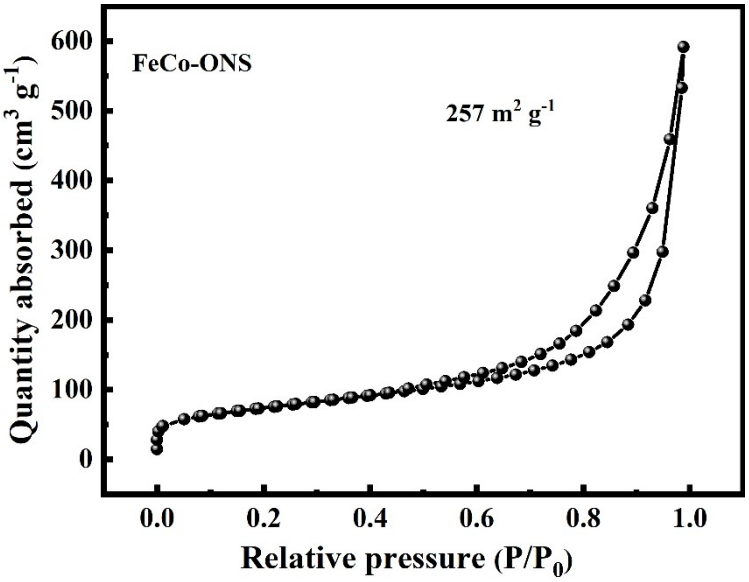

Figure S2. N_2 adsorption-desorption isotherms of FeCo-ONS.

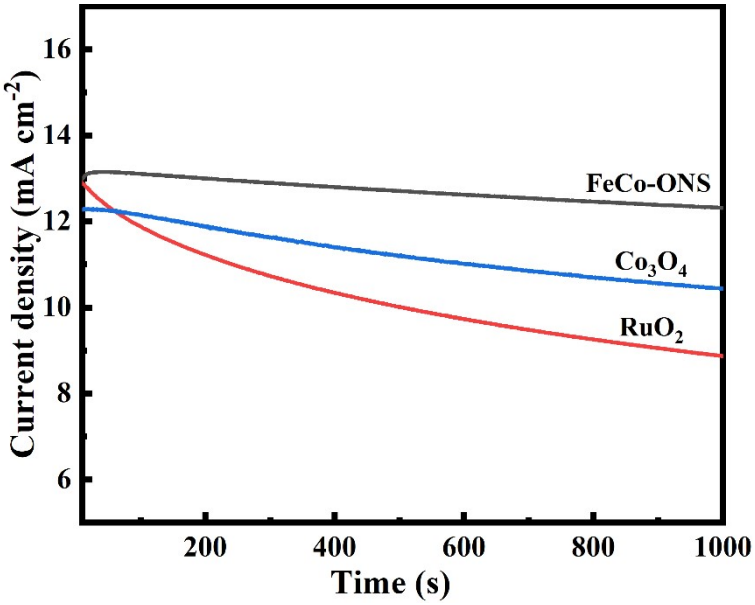

Figure S3. Chronoamperometry curves of FeCo-ONS, RuO_2 and Co_3O_4.

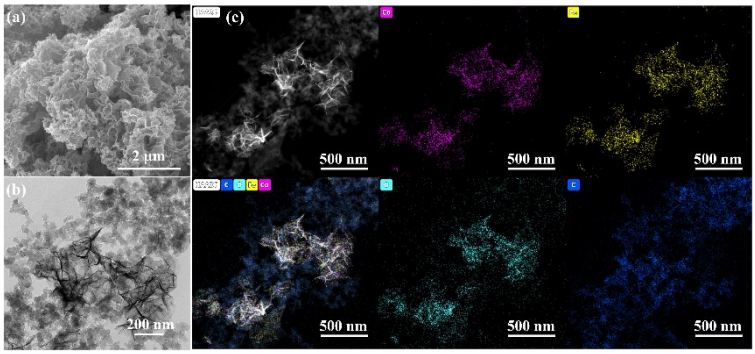

Figure S4. The (a) SEM, (b) TEM and (c) EDS mapping of FeCo-ONS after 2000 CV cycles.

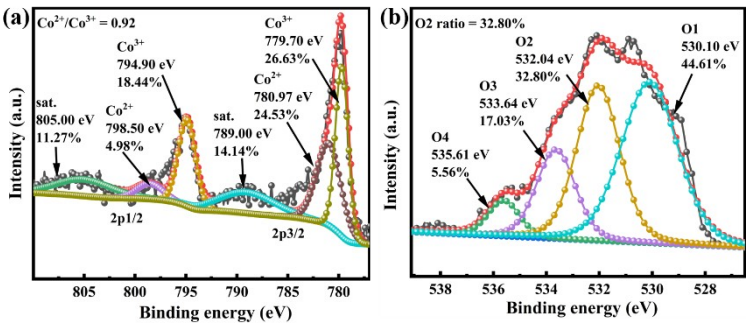

Figure S5. The (a) Co 2p and (b) O 1s XPS spectra of FeCo-ONS after 2000 CV cycles.

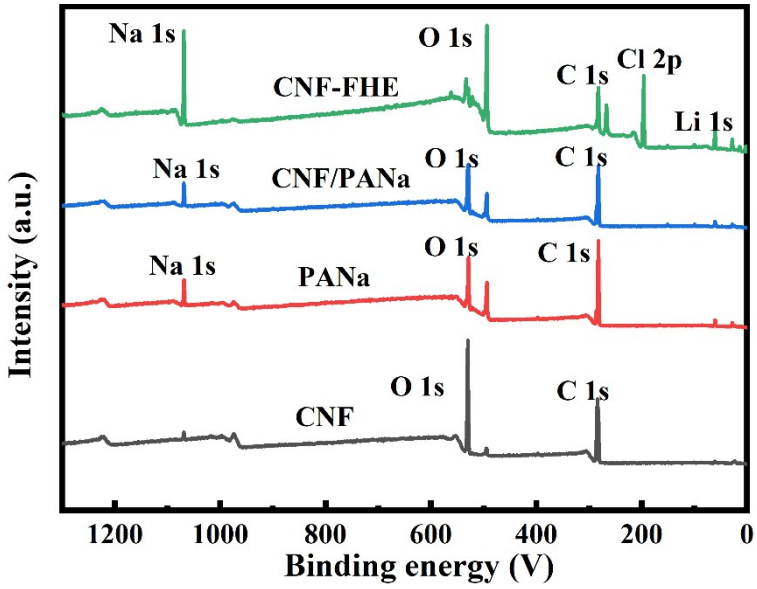

Figure S6. XPS spectra of CNF, PANa, CNF/PANa, CNF-FH.

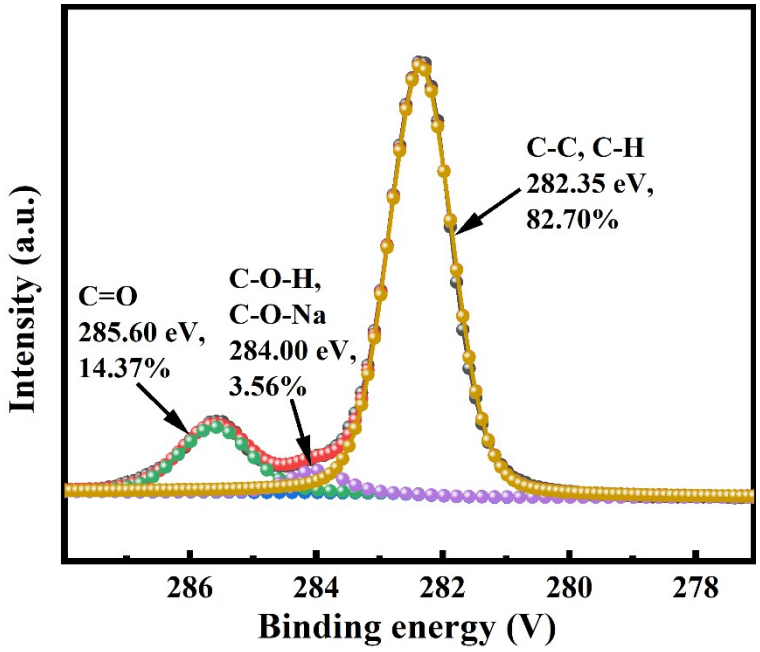

Figure S7. C 1 s XPS spectra of PANa.

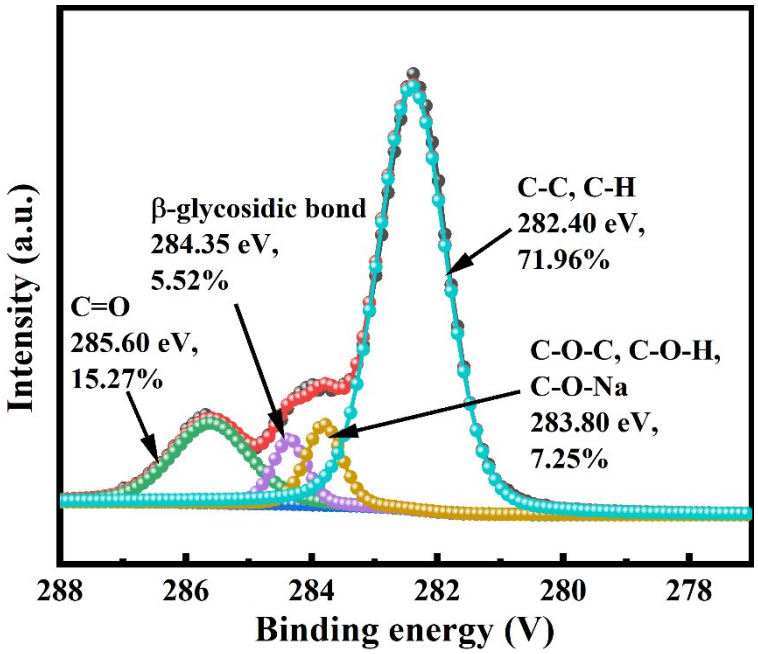

Figure S8. C 1 s XPS spectra of CNF/PANa.

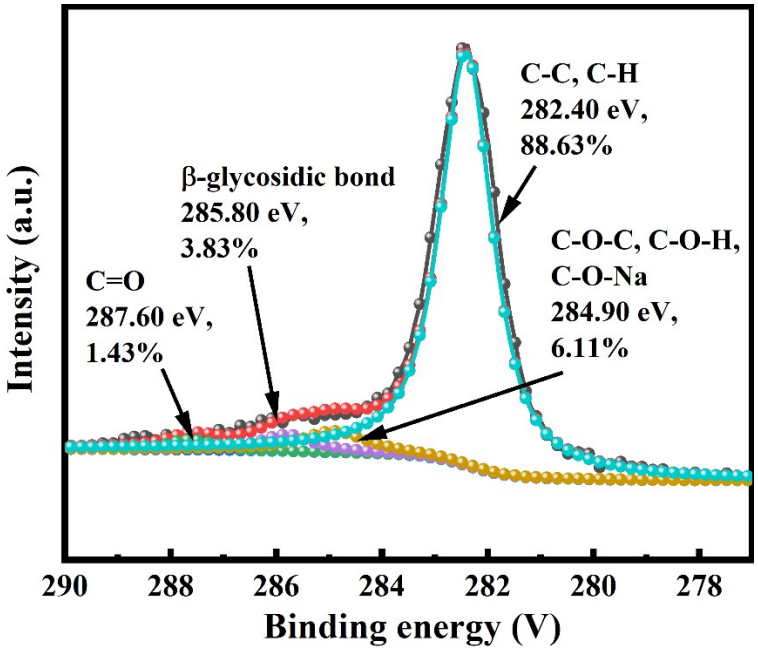

Figure S9. C 1s XPS spectra of CNF-FH.

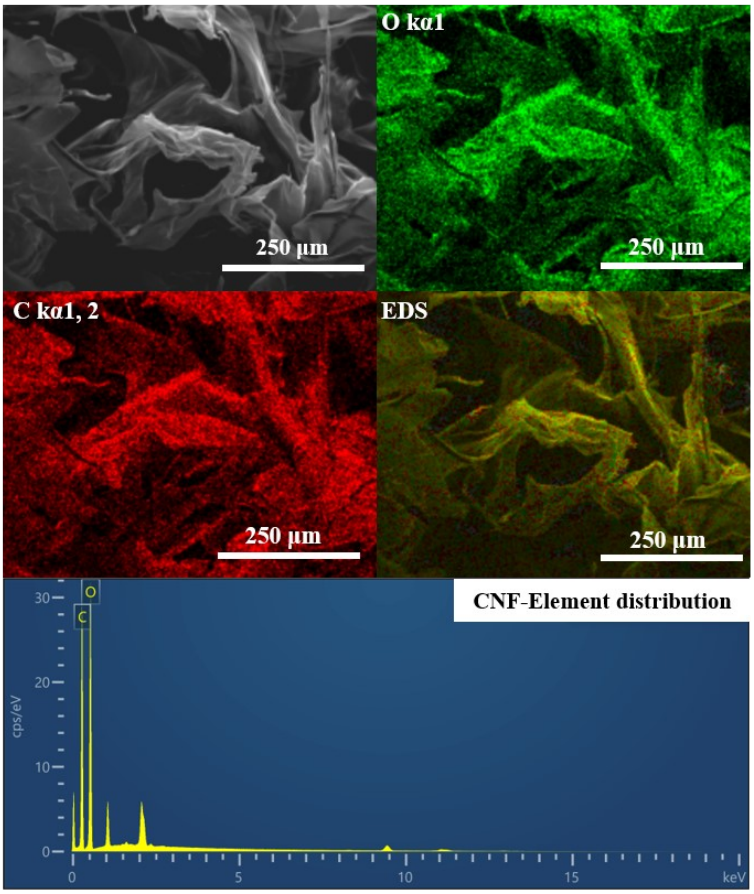

Figure S10. EDS mapping of CNF.

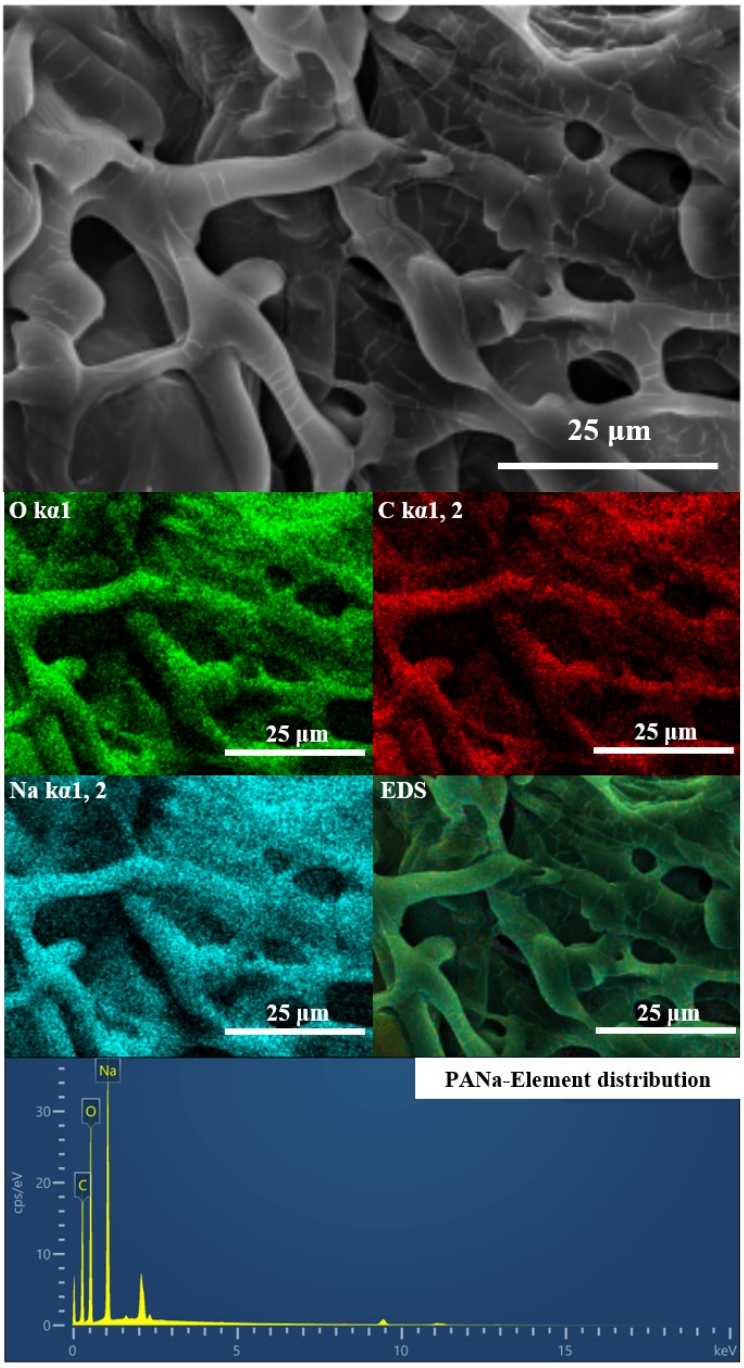

Figure S11. EDS mapping of PANa.

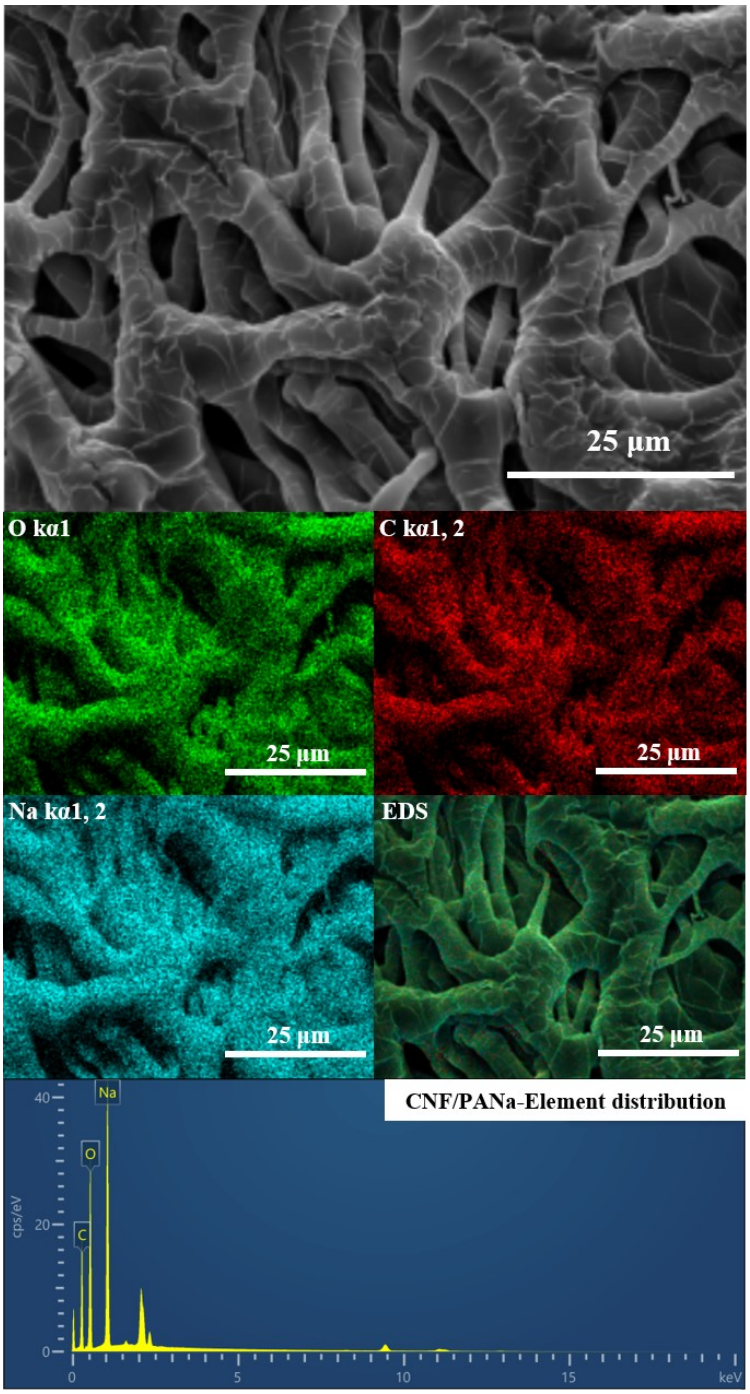

Figure S12. EDS mapping of CNF/PANa.

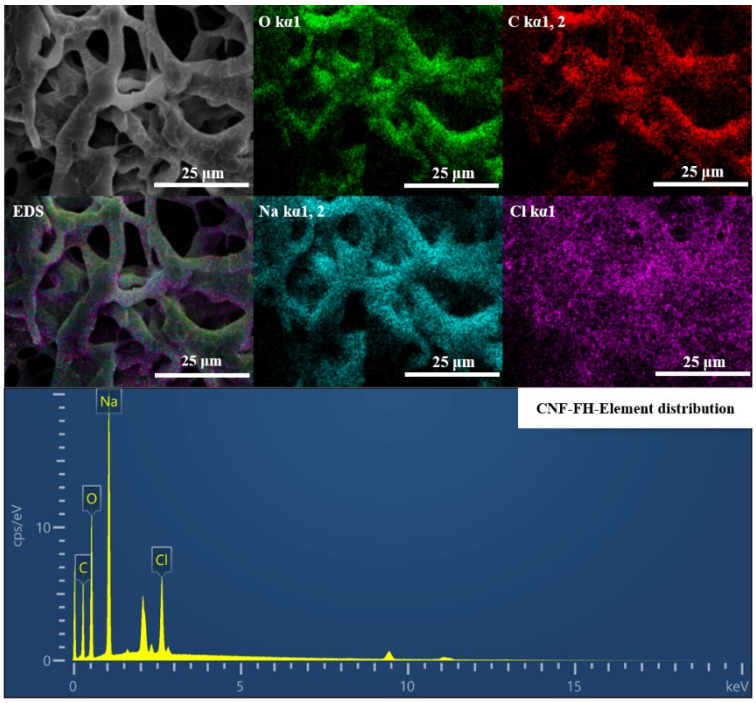

Figure S13. EDS mapping of CNF-FH.

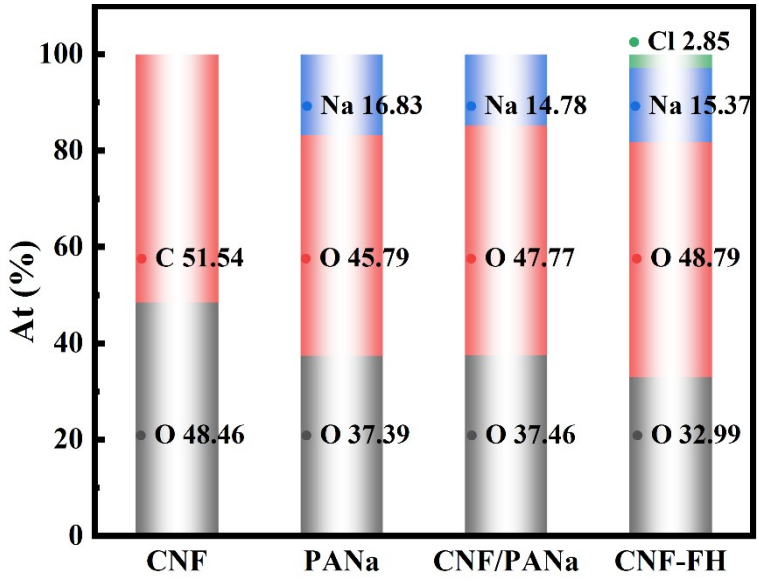

Figure S14. The element distribution of CNF, PANa, CNF/PANa and CNF-FH.

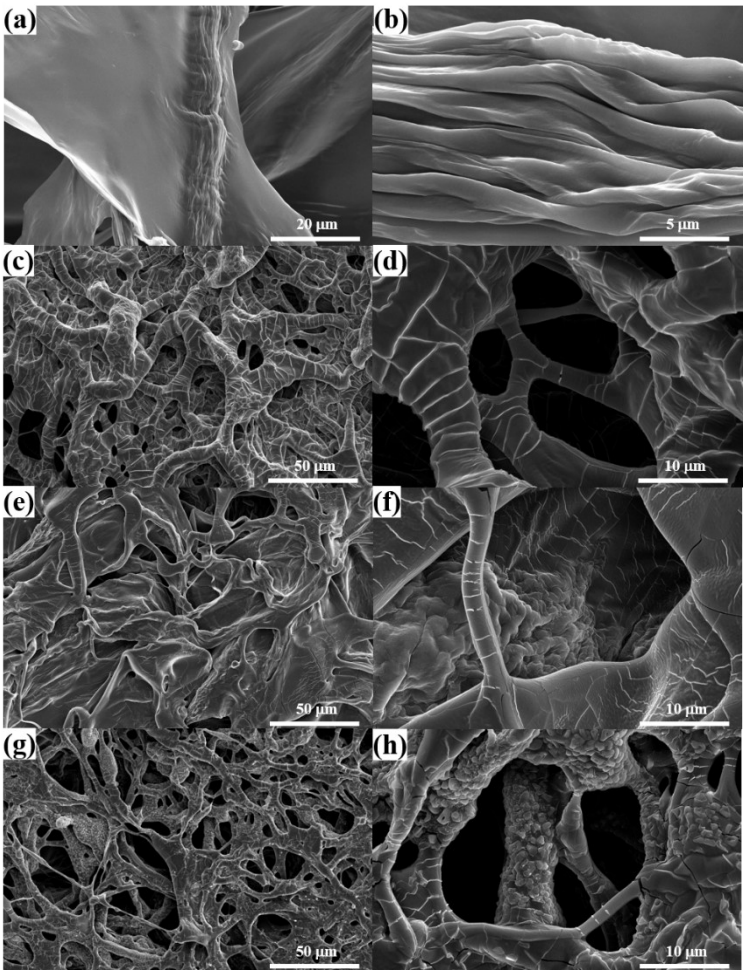

Figure S15. SEM images of freeze-dried (a, b) CNF, (c, d) PANa, (e, f) CNF/PANa and (g, h) CNF-FH.

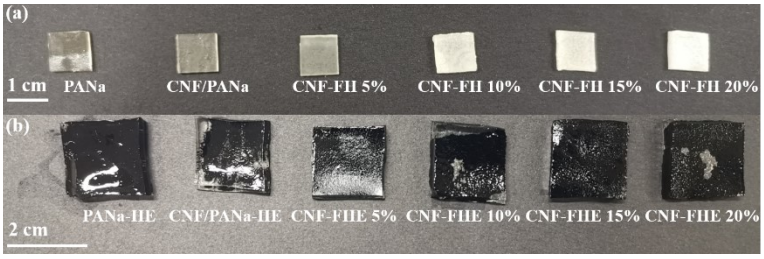

Figure S16. (a) Photos of PANa, CNF/PANa and CNF-FH. (b) Photos of PANa, CNF/PANa and CNF-FH after immersion in 6 M KOH and 0.2 M $ZnAc_2$ solutions.

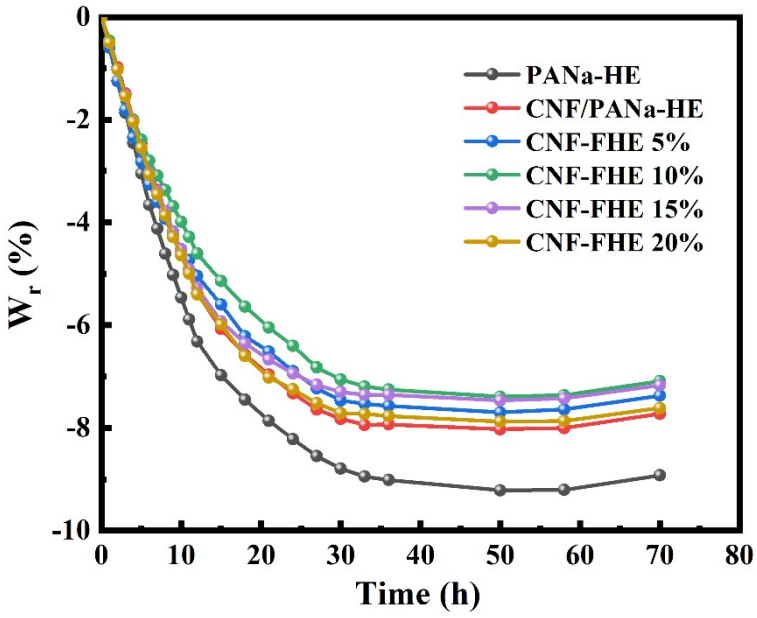

Figure S17. The electrolyte retention capacity at the not-wrapped stated PANa-HE, CNF/PANa-HE and CNF-FHEs.

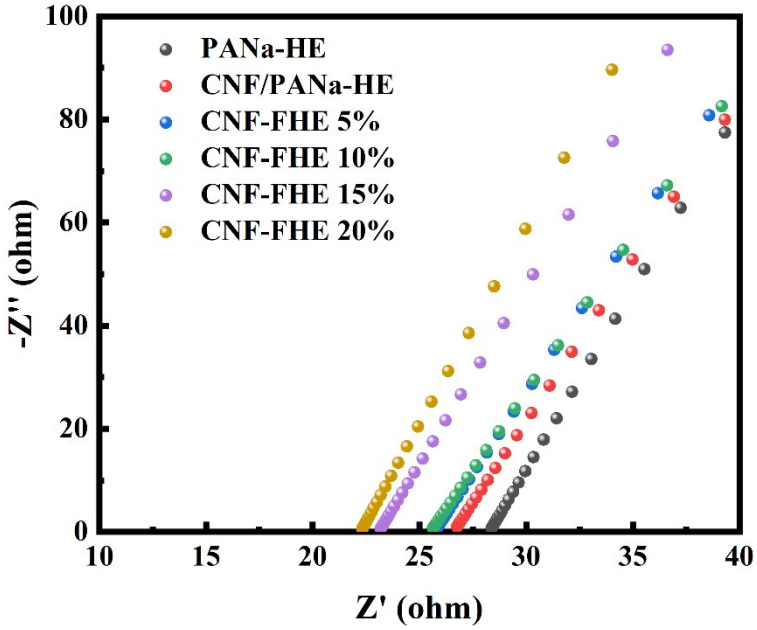

Figure S18. Nyquist plots at -80 °C of PANa, CNF/PANa and CNF-FHEs.

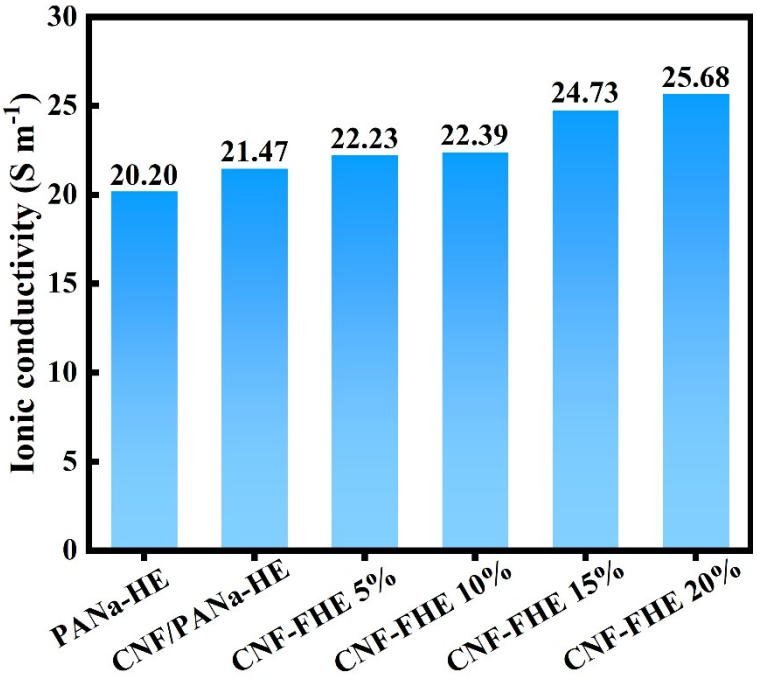

Figure S19. Ionic conductivity at -80 °C of PANa, CNF/PANa and CNF-FHEs.

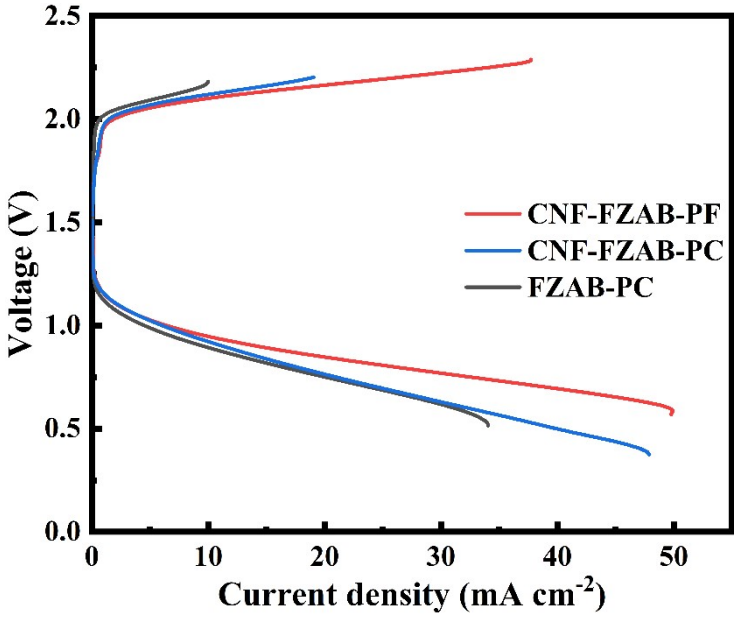

Figure S20. Discharge/charge polarization curves of the FZAB-PC, CNF-FZAB-PC and CNF-FZAB-PF.

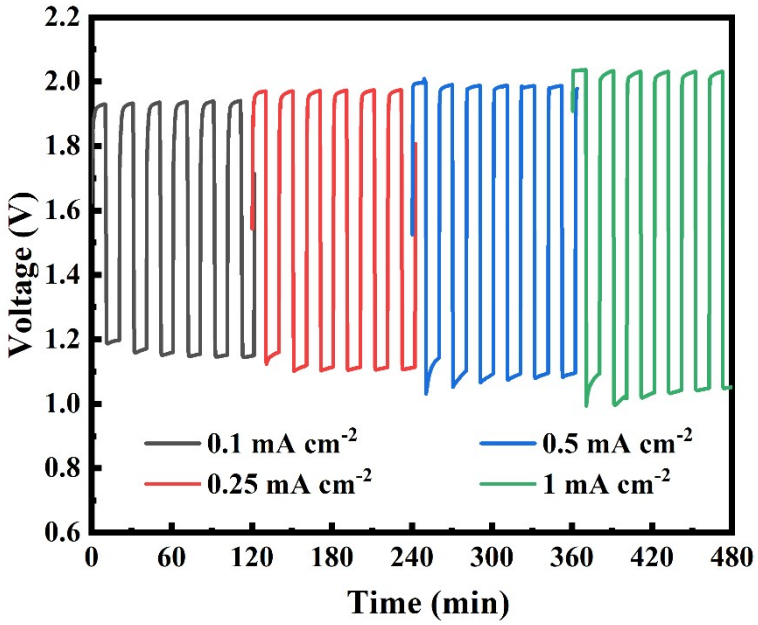

Figure S21. Galvanostatic discharge/charge cycling tests of the CNF-FZAB-PF at 0.1 mA cm^{-2}, 0.25 mA cm^{-2}, 0.5 mA cm^{-2} and 1 mA cm^{-2} with 20 min per cycle.

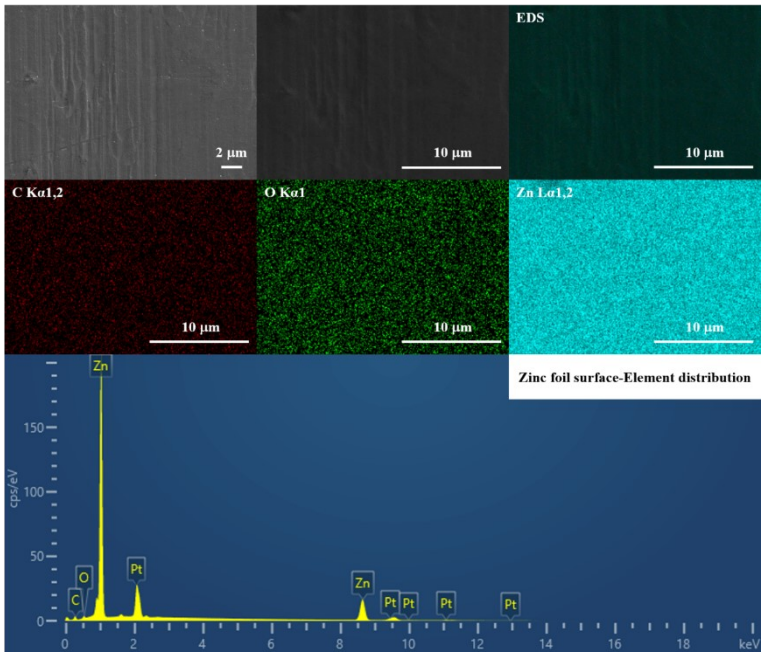

Figure S22. EDS mapping of Zinc foil surface.

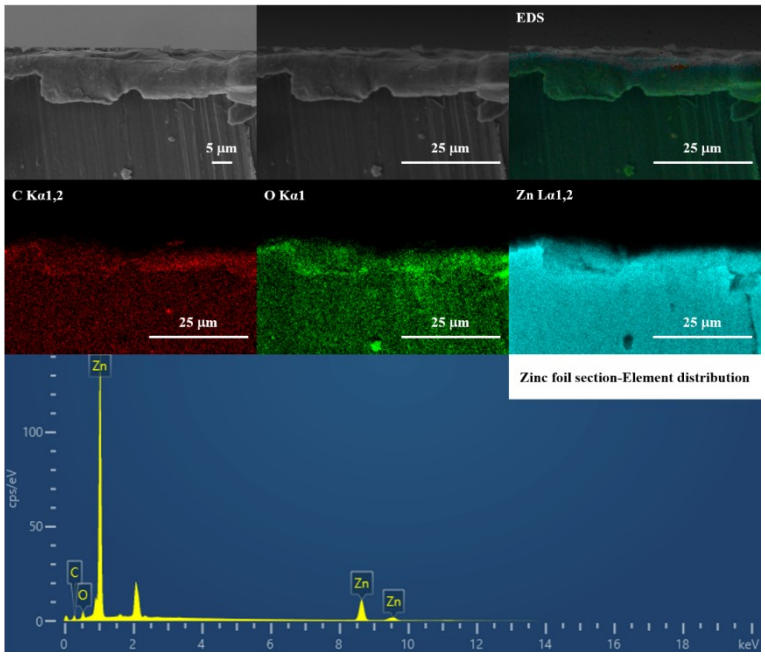

Figure S23. EDS mapping of Zinc foil section.

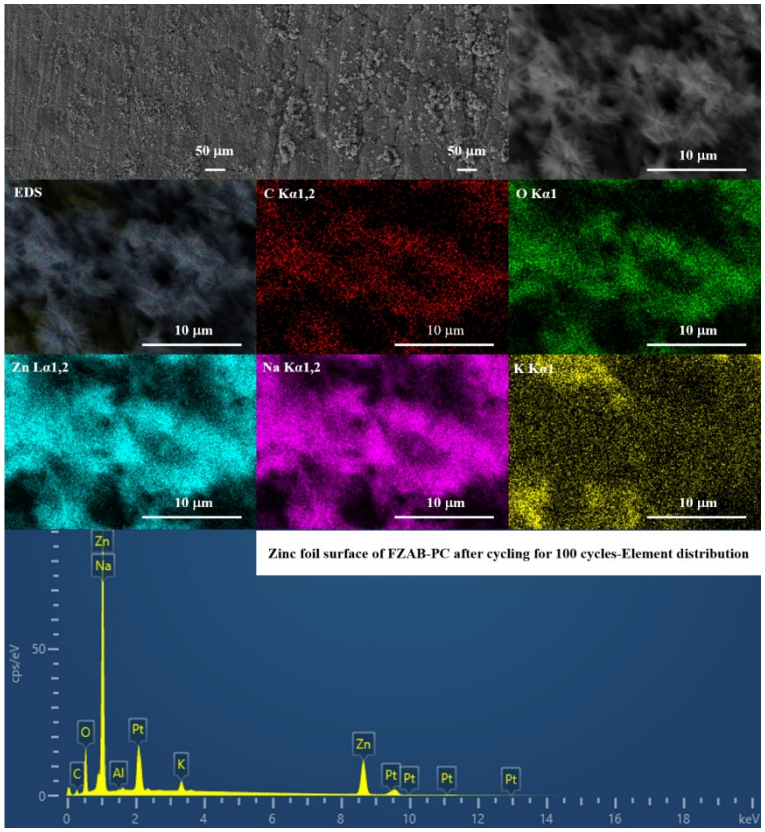

Figure S24. EDS mapping of Zinc foil surface of FZAB-PC after cycling for 100 cycles.

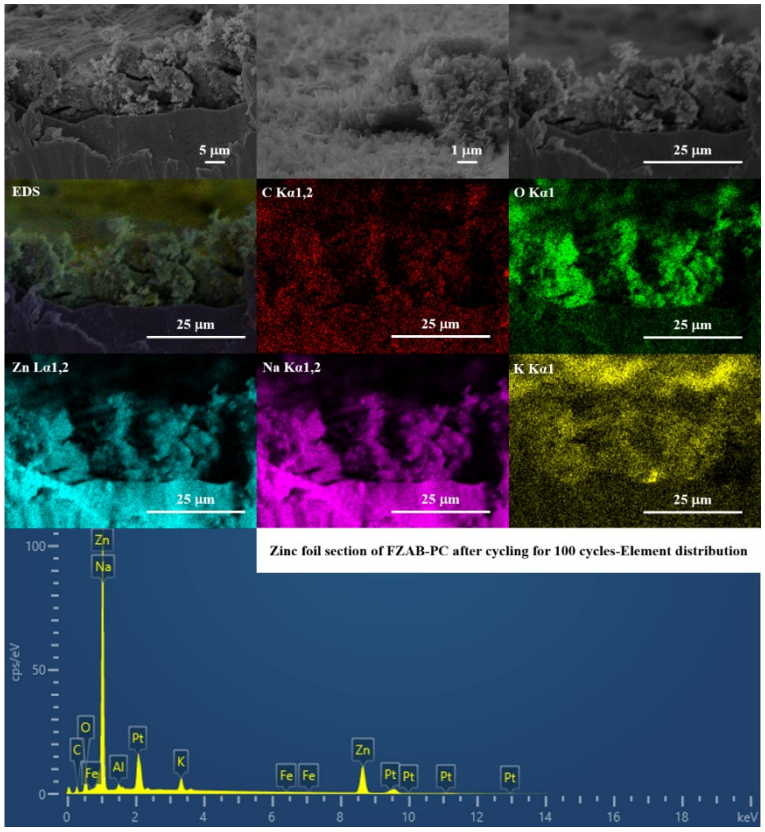

Figure S25. EDS mapping of Zinc foil section of FZAB-PC after cycling for 100 cycles.

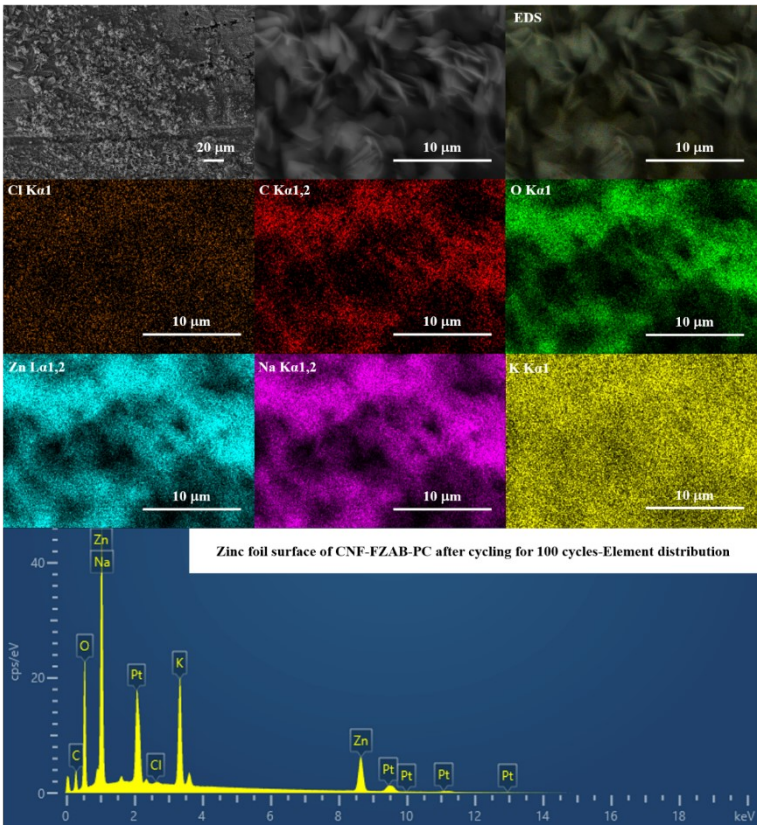

Figure S26. EDS mapping of Zinc foil surface of CNF-FZAB-PC after cycling for 100 cycles.

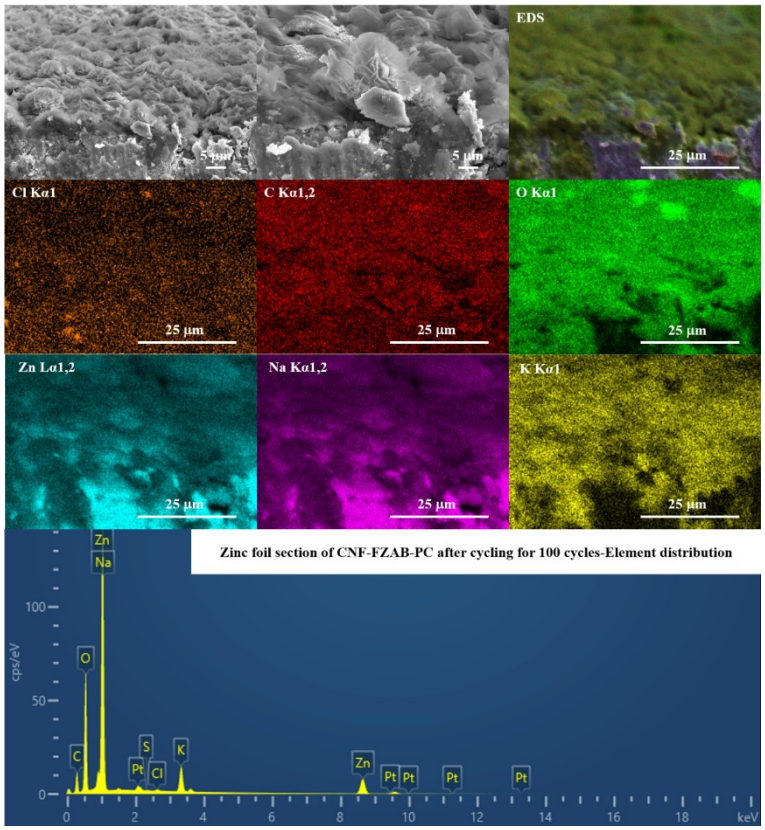

Figure S27. EDS mapping of Zinc foil section of CNF-FZAB-PC after cycling for 100 cycles.

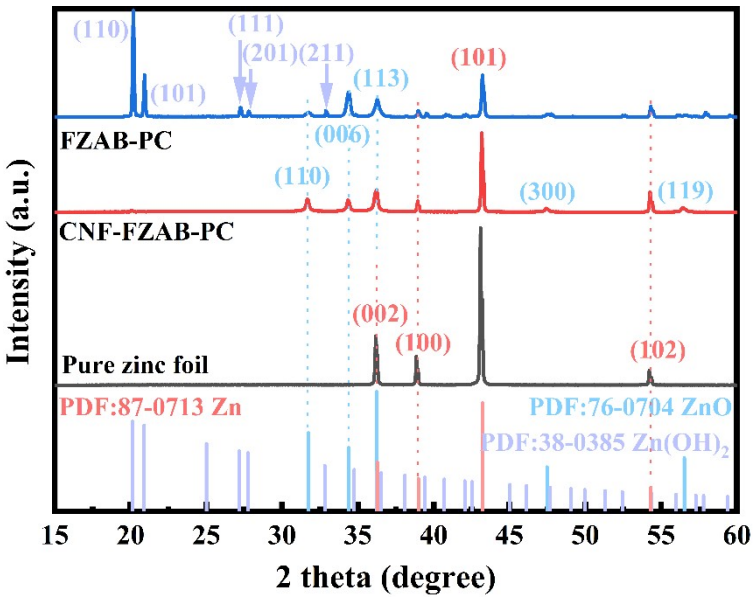

Figure S28. XRD of the zinc anode of zinc foil, FZAB-PC and CNF-FZAB-PC after cycling.